

Decomposition of Ruthenium Olefin Metathesis Catalysts

Soon Hyeok Hong, Anna G. Wenzel,[†] Tina T. Salguero,[‡] Michael W. Day, and Robert H. Grubbs**Contribution from The Arnold and Mabel Beckman Laboratory of Chemical Synthesis, Division of Chemistry and Chemical Engineering, California Institute of Technology, Pasadena, California 91125*

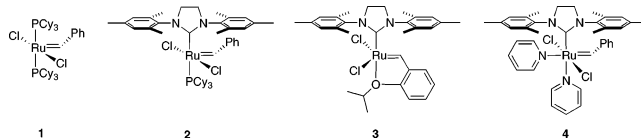
Received February 26, 2007; E-mail: rhg@caltech.edu

Abstract: The decomposition of a series of ruthenium metathesis catalysts has been examined using methyldiene species as model complexes. All of the phosphine-containing methyldiene complexes decomposed to generate methylphosphonium salts, and their decomposition routes followed first-order kinetics. The formation of these salts in high conversion, coupled with the observed kinetic behavior for this reaction, suggests that the major decomposition pathway involves nucleophilic attack of a dissociated phosphine on the methyldiene carbon. This mechanism also is consistent with decomposition observed in the presence of ethylene as a model olefin substrate. The decomposition of phosphine-free catalyst (H₂IMes)(Cl)₂Ru=CH(2-C₆H₄-O-*i*-Pr) (H₂IMes = 1,3-dimesityl-4,5-dihydroimidazol-2-ylidene) with ethylene was found to generate unidentified ruthenium hydride species. The novel ruthenium complex (H₂IMes)-(pyridine)₃(Cl)₂Ru, which was generated during the synthetic attempts to prepare the highly unstable pyridine-based methyldiene complex (H₂IMes)(pyridine)₂(Cl)₂Ru=CH₂, is also reported.

Introduction

Over the past decade, olefin metathesis has emerged as a powerful method for the formation of carbon–carbon double bonds.^{1,2} In particular, ruthenium olefin metathesis catalysts **1–4** have been used extensively in organic and polymer chemistry due to their high activity and functional group tolerance.^{3–6} Despite these advances, one of the major limiting factors for the use of ruthenium carbene catalysts in many reactions is the lifetime and efficiency of these catalysts. As a result, the ring-closing of large rings requires increased catalyst loadings in high-dilution conditions, and the metathesis of highly substituted and/or electron-deficient olefins still requires elevated temperatures and extended reaction times.^{7–10} Furthermore, catalyst decomposition sometimes leads to unwanted side reactions, such as olefin isomerizations.^{11–14} As identified in previous work,

the key to catalyst efficiency is the ratio of the rate of olefin metathesis relative to that of catalyst decomposition.¹⁵ Thus, to rationally design a more efficient catalyst for olefin metathesis, it is essential to understand the decomposition pathways of existing catalysts.



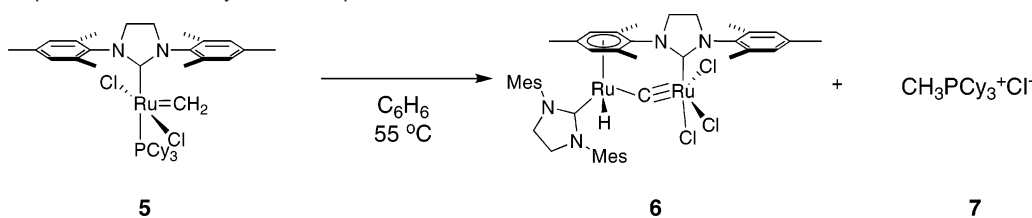
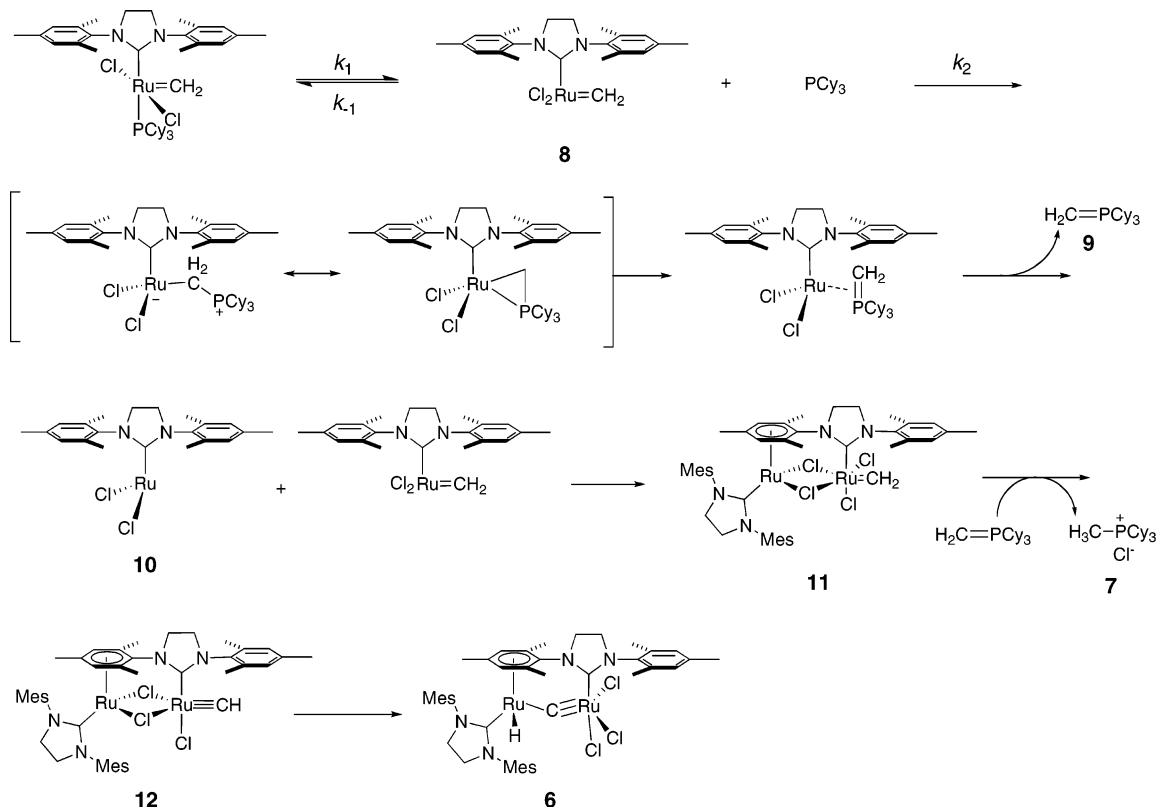
Despite the importance of mechanistic elucidation to catalyst optimization, relatively few studies have been performed to understand the decomposition pathways of ruthenium-based metathesis systems. Mol and co-workers reported that the degradation of **1** and **2** with primary alcohols produced RuClH(CO)(L)(PCy₃) (L = *N*-heterocyclic carbene (NHC) or PCy₃) complexes.^{16–18} Diver and co-workers reported carbon monoxide-promoted benzylidene or methyldiene insertion into a mesityl group of complex **2** or **5**.¹⁹ Van Rensburg and co-workers have suggested a substrate-induced decomposition mechanism for these catalysts based on DFT calculations involving a β -hydride transfer from a ruthenacyclobutane intermediate.²⁰ Our group has reported the insertion of ruthenium into the C–H bond of

[†] Current address: Joint Science Department; Claremont McKenna, Pitzer and Scripps Colleges; Claremont, CA 91711.

[‡] Current address: HRL Laboratories, LLC; Malibu, CA 90265-4797.

- Ivin, K. J.; Mol, J. C. *Olefin Metathesis and Metathesis Polymerization*; Academic Press: San Diego, CA, 1997.
- Grubbs, R. H. *Tetrahedron* **2004**, *60*, 7117–7140.
- Fürstner, A. *Angew. Chem., Int. Ed.* **2000**, *39*, 3012–3043.
- Frenzel, U.; Nuyken, O. *J. Polym. Sci., Part A: Polym. Chem.* **2002**, *40*, 2895–2916.
- Han, S.-Y.; Chang, S. In *Handbook of Metathesis*; Grubbs, R. H., Ed.; Wiley-VCH: Weinheim, Germany, 2003; Vols. 1–3.
- Trnka, T. M.; Grubbs, R. H. *Acc. Chem. Res.* **2001**, *34*, 18–29.
- Grubbs, R. H. *Tetrahedron* **2004**, *60*, 7117–7140.
- Nicola, T.; Brenner, M.; Donsbach, K.; Kreye, P. *Org. Process Res. Dev.* **2005**, *9*, 513–515.
- Vinokurov, N.; Michrowska, A.; Szmigielska, A.; Drzazga, Z.; Wójcicki, G.; Demchuk, O. M.; Grela, K.; Pietrusiewicz, K. M.; Butenschön, H. *Adv. Synth. Catal.* **2006**, *348*, 931–938.
- Martin, W. H. C.; Bleichert, S. *Curr. Top. Med. Chem.* **2005**, *5*, 1521–1540.
- Alcaide, B.; Almendros, P. *Chem. Eur. J.* **2003**, *9*, 1259–1262.
- Schmidt, B. *Eur. J. Org. Chem.* **2004**, 1865–1880.

- Hong, S. H.; Sanders, D. P.; Lee, C. W.; Grubbs, R. H. *J. Am. Chem. Soc.* **2005**, *127*, 17160–17161.
- Courchay, F. C.; Sworen, J. C.; Ghiviriga, I.; Abboud, K. A.; Wagener, K. B. *Organometallics* **2006**, *25*, 6074–6086.
- Ulman, M.; Grubbs, R. H. *J. Org. Chem.* **1999**, *64*, 7202–7207.
- Banti, D.; Mol, J. C. *J. Organomet. Chem.* **2004**, *689*, 3113–3116.
- Dinger, M. B.; Mol, J. C. *Eur. J. Inorg. Chem.* **2003**, 2827–2833.
- Dinger, M. B.; Mol, J. C. *Organometallics* **2003**, *22*, 1089–1095.
- Galan, B. R.; Gembicky, M.; Dominiak, P. M.; Keister, J. B.; Diver, S. T. *J. Am. Chem. Soc.* **2005**, *127*, 15702–15703.

Scheme 1. Decomposition of the Methylidene Complex **5****Scheme 2.** Proposed Decomposition Mechanism

one of the methyl groups on the NHC ligand that can occur during the preparation of **2**.²¹ However, the lack of well-characterized decomposition products under typical metathesis conditions has limited the understanding of the decomposition mechanism overall.

Ruthenium methylidenes serve as critical intermediates in most metathesis reactions, such as ring-closing metathesis (RCM), cross metathesis (CM), and acyclic diene metathesis (ADMET) reactions. However, these intermediates also rank among the least stable isolable species.¹⁵ A thorough understanding of methylidene decomposition and stability is crucial to the design of more stable catalyst systems.^{15,22,23} In a preliminary communication, we showed that methylidene complex **5** decomposed to form the dinuclear ruthenium hydride complex **6** and methyltricyclohexylphosphonium chloride (**7**) (Scheme 1).²² On the basis of the observation of **6** and **7** and the results of kinetic experiments, we proposed that complex **5**

decomposes via the nucleophilic attack of a dissociated phosphine on the methylidene carbon (Scheme 2). This decomposition study has now been expanded to include other ruthenium-based olefin metathesis catalysts, including the phosphine-free catalysts **3** and **4**.

Results and Discussion

Decomposition of Phosphine-Based Catalysts. Catalyst decomposition rates were determined using ¹H NMR spectroscopy by following the diminution of the ruthenium methylidene resonance integral over time.¹⁵ Recrystallization and spectroscopic methods were used to identify and characterize decomposition products. All of the tested methylidene complexes of phosphine-based ruthenium catalysts decomposed to generate methyltricyclohexylphosphonium salts as the major phosphine species (Table 1).²⁴ In our previous report, we were not able to conclusively identify the phosphine product from the decomposition of complex **13**. In this case, the phosphine activation was proposed on the basis of the ²H NMR study with (PCy₃)₂-Cl₂Ru=CD₂ (**13-d**).¹⁵ Here the product has been characterized successfully as CH₃PCy₃⁺Cl⁻ (**7**) by comparison with an

(20) van Rensburg, W. J.; Steynberg, P. J.; Meyer, W. H.; Kirk, M. M.; Forman, G. S. *J. Am. Chem. Soc.* **2004**, *126*, 14332–14333.

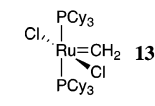
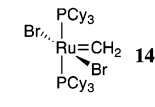
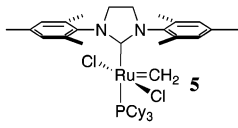
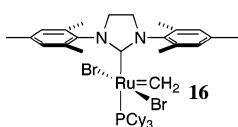
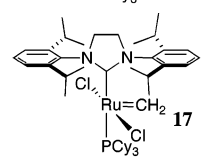
(21) Trnka, T. M.; Morgan, J. P.; Sanford, M. S.; Wilhelm, T. E.; Scholl, M.; Choi, T. L.; Ding, S.; Day, M. W.; Grubbs, R. H. *J. Am. Chem. Soc.* **2003**, *125*, 2546–2558.

(22) Hong, S. H.; Day, M. W.; Grubbs, R. H. *J. Am. Chem. Soc.* **2004**, *126*, 7414–7415.

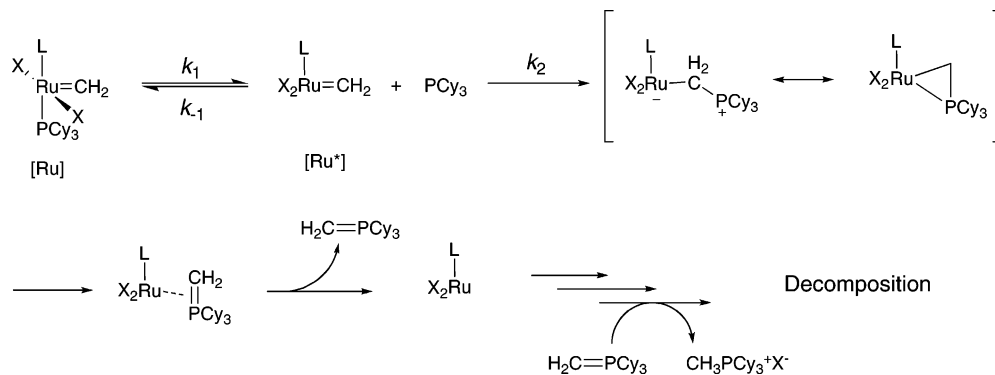
(23) Sanford, M. S.; Love, J. A.; Grubbs, R. H. *J. Am. Chem. Soc.* **2001**, *123*, 6543–6554.

(24) See Supporting Information for kinetic plots and ³¹P spectra after catalyst decomposition.

Table 1. Decomposition of Ruthenium Methylidene Complexes^a

Entry	Methylidenes	Half-Life	k_{decomp} (s ⁻¹)	Decomposition Products (Conversion) ^b
1		40 min	0.016	CH ₃ PCy ₃ ⁺ Cl ⁻ (82%)
2		35 min	0.018	CH ₃ PCy ₃ ⁺ Br ⁻ (15 , 85%)
3		5 h 40 min	0.0021	6 (46%) ^c CH ₃ PCy ₃ ⁺ Cl ^{-d}
4		5 h 15 min	0.0024	CH ₃ PCy ₃ ⁺ Br ^{-d}
5		1 h	0.011	CH ₃ PCy ₃ ⁺ Cl ⁻ (81%) H ₂ IPr ⁺ H ⁻ Cl ^{-e}

^a Conditions: 0.023 M, C₆D₆, 55 °C, anthracene as an internal standard. ^b Determined by ¹H NMR spectroscopy. ^c Isolated yield. ^d Conversions could not be determined. ^e H₂IPr = 1,3-bis(2,6-diisopropylphenyl)-4,5-dihydroimidazol-2-ylidene.

Scheme 3. Phosphine Dissociation and Attack Mechanism

independently prepared sample of the salt (¹H, ¹³C, and HRMS). The ²H peak observed at ~2.5 ppm during the decomposition of **13-d₂** has also been demonstrated to originate from the methyl protons of CD₃PCy₃⁺Cl⁻ (**7-d₃**).

The conversions to the phosphine products CH₃PCy₃⁺X⁻ were determined by comparing the ¹H NMR integration of the α-proton in the cyclohexyl rings of the phosphonium salts with an internal standard (anthracene). The conversions were high, 81–85%, for (PCy₃)₂Cl₂Ru=CH₂ (**13**), (PCy₃)₂Br₂Ru=CH₂ (**14**), and (H₂IPr)(PCy₃)Cl₂Ru=CH₂ (**17**) (Table 1, entries 1, 2, and 5) (H₂IPr = 1,3-bis(2,6-diisopropylphenyl)-4,5-dihydroimidazol-2-ylidene). For (H₂IMes)(PCy₃)Cl₂Ru=CH₂ (**5**) and (H₂IMes)(PCy₃)Br₂Ru=CH₂ (**16**) (entries 3 and 4) (H₂IMes = 1,3-dimesityl-4,5-dihydroimidazol-2-ylidene), the conversions could not be determined because of peak overlap, although ³¹P NMR spectra indicate methyltricyclohexylphosphonium salts are the major phosphine-containing products.²⁴ These observed conversions strongly suggest that phosphine is involved in the major decomposition pathway for the ruthenium methylidene complexes listed in Table 1.

The decompositions of phosphine-based ruthenium methylidene complexes were found to follow first-order kinetics; the decomposition rates were not affected by the addition of excess phosphine.^{15,22,23} As anticipated, catalysts containing an *N*-heterocyclic carbene ligand had increased lifetimes compared with bis(phosphine)-based catalysts.^{22,25,26} Changing the chloride ligands to bromides was found to only slightly decrease the catalyst lifetimes. Attempts to replace the chloride ligands with iodides were unsuccessful, presumably due to an increased rate of decomposition.²³

Complexes bearing H₂IPr ligands, such as **17**, are known to initiate very quickly in olefin metathesis reactions because of the steric bulk of the *N*-heterocyclic carbene ligand.^{27,28} However, methylidene complex **17** is much less stable than the H₂IMes derivatives **5** and **16** (entries 3 and 4). The phosphine

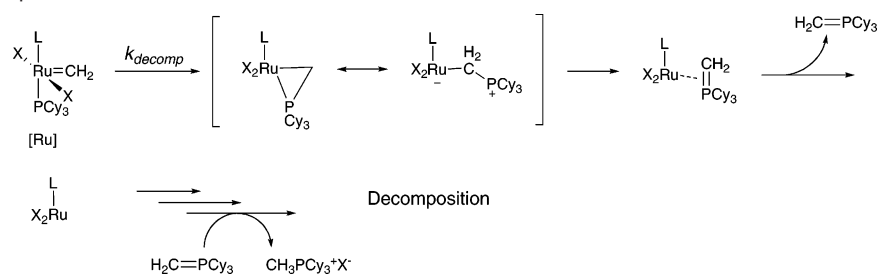
(25) Ulman, M. Ph.D. Dissertation, California Institute of Technology, 2000.

(26) Huang, J. K.; Schanz, H. J.; Stevens, E. D.; Nolan, S. P. *Organometallics* **1999**, *18*, 5375–5380.

(27) Fürstner, A.; Ackermann, L.; Gabor, B.; Goddard, R.; Lehmann, C. W.; Mynott, R.; Stelzer, F.; Thiel, O. R. *Chem. Eur. J.* **2001**, *7*, 3236–3253.

(28) Dinger, M. B.; Mol, J. C. *Adv. Synth. Catal.* **2002**, *344*, 671–677.

Scheme 4. Internal Phosphine Attack Mechanism



ligand of **17** dissociates faster than the phosphine of **5** or **16**, which increases the concentration of free phosphine and thus accelerates phosphine attack on the methylidene carbon.²⁹ This result indicates that a mechanism involving phosphine dissociation and attack (Scheme 3) is more reasonable than a mechanism involving the internal attack of phosphine (Scheme 4).

It was difficult to experimentally distinguish these two possible mechanisms, as both kinetic expressions are identical and consistent with the lack of rate dependence on phosphine concentration and the first-order kinetic behavior that was observed (eq 1³⁰ for the mechanism in Scheme 3 and eq 2 for

$$\text{rate of decomposition} = k_2[\text{Ru}^*][\text{PCy}_3] = \frac{k_1 k_2 [\text{Ru}][\text{PCy}_3]}{k_{-1}[\text{PCy}_3] + k_2[\text{PCy}_3]} = \frac{k_1 k_2}{k_{-1} + k_2} [\text{Ru}] \quad (1)$$

$$\text{rate of decomposition} = k_{\text{decomp}}[\text{Ru}] \quad (2)$$

the mechanism in Scheme 4). Experiments, such as the addition of more nucleophilic phosphines like trimethylphosphine, were unsuccessful presumably due to phosphine-exchange of the ruthenium methylidenes.³¹ However, if decomposition occurs via the internal attack of phosphine onto the methylidene carbon, the decomposition rates of complex **5**, **16**, and **17** should not be so much different considering similar electronic properties between H₂IMes and H₂IPr ligands.³² Because it is not, we favor the mechanism involving the nucleophilic attack of free phosphine for the decomposition of ruthenium methylidene complexes (Scheme 3). The nucleophilic attack of phosphines on the carbene carbon of ruthenium alkylidenes has also been reported by Hofmann and co-workers.³³

Decomposition in the Presence of Ethylene. Van Rensburg and co-workers have reported the substrate-induced decomposition of **5** and **13** using ethylene as a model substrate.²⁰ On the basis of theoretical and experimental results, they proposed that decomposition of **5** in the presence of ethylene could occur via a ruthenium allyl species formed by β -hydrogen abstraction from the corresponding ruthenacyclobutane intermediate. Reductive elimination then yields propene as the major olefinic compound. However, they were not able to characterize the major phosphine

decomposition product. We have re-examined this reaction and found that ³¹P NMR spectra of decomposed samples reveal a major phosphine complex at 34.6 ppm after decomposition of both **5** and **13** (Figure 1), which corresponds to CH₃PCy₃⁺Cl⁻. The identity of this species was confirmed by spectroscopic methods. The ¹³C NMR spectrum, which shows a characteristic doublet for the phosphonium salt's methyl protons at 1.5 ppm, was particularly revealing.²² From this evidence, we believe that phosphine attack on the methylidene carbon is also a major pathway in the decomposition of **5** and **13** in the presence of ethylene.

Further evidence for catalyst decomposition by phosphine attack on the methylidene carbon and the subsequent generation of complex **11** (Scheme 2) was found in conducting a series of experiments on catalyst **18**,³⁴ the triphenylphosphine analogue of **2**, in the presence of ethylene (Scheme 5). Rapid conversion to a new alkylidene species at 18.59 ppm was observed by ¹H NMR upon the exposure of a 0.035 M solution of **18** in dichloromethane-*d*₂ to an atmosphere of ethylene at 23 °C. However, in contrast to reactions conducted using catalyst **2**, where methylidene **5** was initially observed,²³ this new alkylidene species was found not to be the triphenylphosphine-ligated methylidene, which was present in only trace amounts (<2%). Attempts to characterize the new alkylidene species were hampered by its instability; the use of an internal standard indicated that the maximum conversion to this unidentified complex was approximately 33% after 8 min (83% conversion of **18**), which rapidly decreased to ~2% after 120 min.³⁵ Interestingly, the only product visible by ³¹P NMR spectroscopy upon the complete consumption of alkylidene was methyltriphenylphosphonium chloride (23.0 ppm), indicating that no phosphine remained bound to the ruthenium and that a

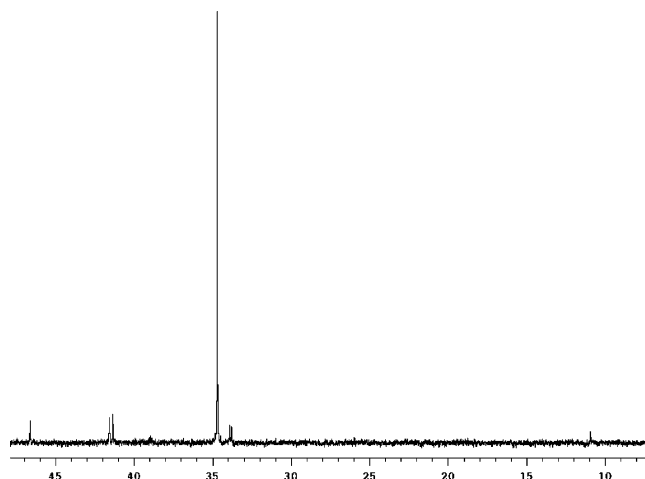


Figure 1. ³¹P NMR spectrum of the decomposition of **13** in the presence of ethylene.

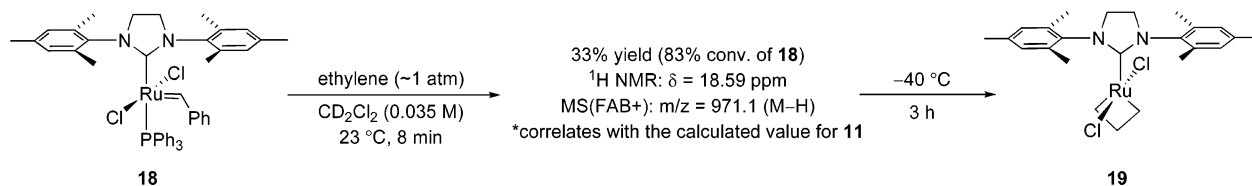
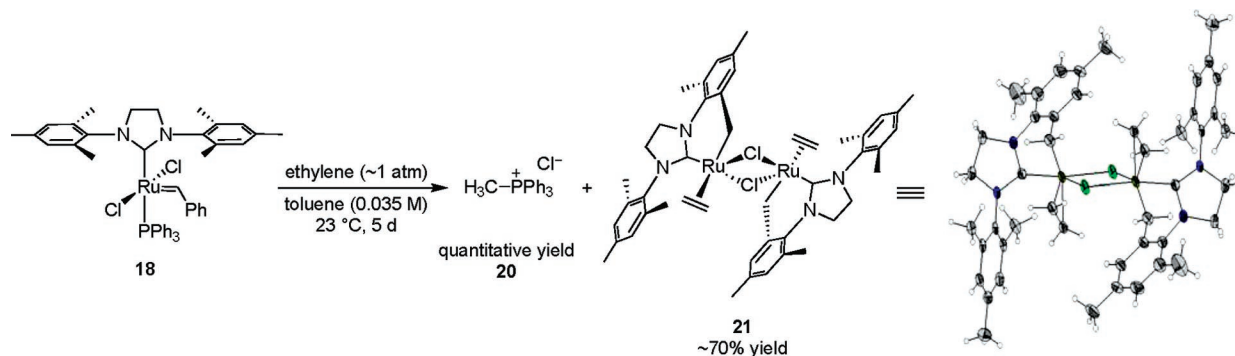
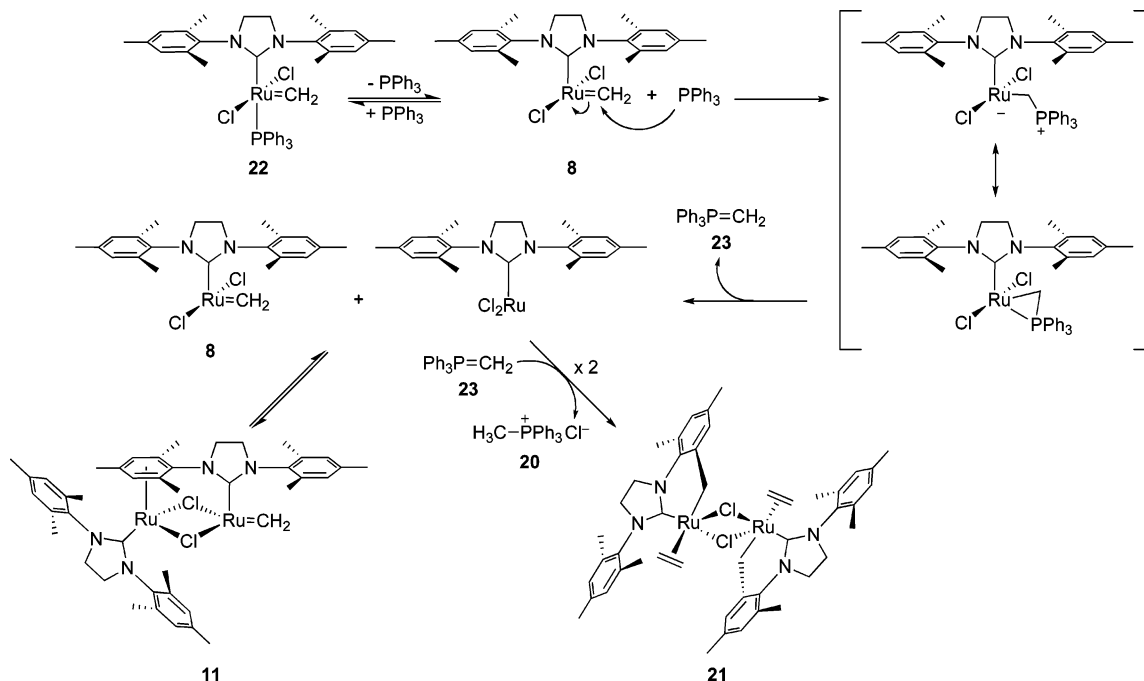
(29) Courchay, F. C.; Sworen, J. C.; Wagener, K. B. *Macromolecules* **2003**, *36*, 8231–8239.

(30) Steady-state approximation was applied to eq 1.

(31) Several unidentified phosphorus peaks were observed in ³¹P NMR spectra from the reaction between **5** and PMe₃.

(32) We think that the internal attack of PCy₃ will be less affected by the steric hindrance of H₂IPr ligands and the geometry is not favorable for the internal attack. For the electronic properties of *N*-heterocyclic carbene ligands, see: Dorta, R.; Stevens, E. D.; Scott, N. M.; Costabile, C.; Cavallo, L.; Hoff, C. D.; Nolan, S. P. *J. Am. Chem. Soc.* **2005**, *127*, 2485–2495.

(33) Hansen, S. M.; Rominger, F.; Metz, M.; Hofmann, P. *Chem. Eur. J.* **1999**, *5*, 557–566.

Scheme 5. Reaction of Catalyst **18** with Ethylene**Scheme 6.** Isolation of the Major Decomposition Product in the Reaction of **18** with Ethylene**Scheme 7.** Proposed Mechanistic Pathway for the Decomposition of the Methylidene of **18** with Ethylene

decomposition process similar to that of catalyst **5** might be in effect. However, complex **6** was not observed in the reaction mixture, suggesting a divergent mechanistic pathway. Mass spectrometric analysis (FAB⁺) of the reaction mixture at 8 min identified a ruthenium species with a m/z of 971.1, supporting the identity of the intermediate alkylidene to be complex **11**, a species that had originally been proposed in the decomposition of **5** but not observed (Scheme 2).²² This intermediate appears to be capable of reverting back to a 14-electron methylidene species, based on the observation that decreasing the temperature of a reaction mixture containing **11** to -40 °C in the presence of ethylene was found to generate metallacycle **19**.^{36–38} It is

important to note that catalyst **18** does not react with ethylene at this temperature.

The major decomposition product of **18** with ethylene ultimately was identified by running the reaction in Scheme 5 on a $77 \mu\text{mol}$ scale in toluene. After 5 days at 23 °C, methyltriphenylphosphonium chloride was isolated in quantitative yield, in addition to 52 mg of a red-brown, crystalline solid that was found to be unstable in solution in the absence of ethylene. X-ray analysis determined the crystal structure

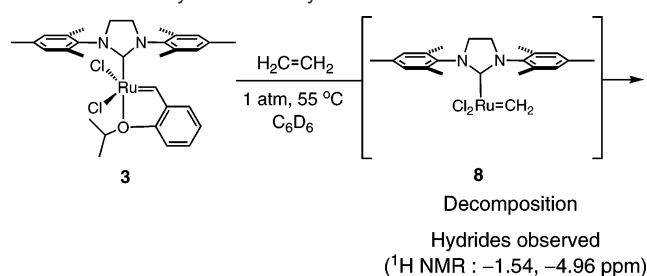
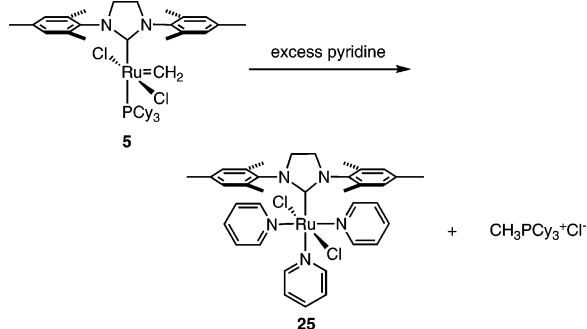
(34) Sanford, M. S.; Love, J. A.; Grubbs, R. H. *Organometallics* **2001**, *20*, 5314–5318.

(35) Values correspond to NMR yields utilizing anthracene (0.014 M) as an internal reaction standard. Alkylidene assumed to be methylidene-derived (2H); conversion based on Ru is 66% if it is assumed that the complex is the bis-ruthenium complex **11**.

(36) Romero, P. E.; Piers, W. E. *J. Am. Chem. Soc.* **2005**, *127*, 5032–5033.

(37) Wenzel, A. G.; Grubbs, R. H. *J. Am. Chem. Soc.* **2006**, *128*, 16048–16049.

(38) Romero, P. E.; Piers, W. E. *J. Am. Chem. Soc.* **2007**, *129*, 1698–1704.

Scheme 8. Catalyst **3** with Ethylene**Scheme 9.** Formation of (H₂IMes)(py)₃(Cl)₂Ru (**25**)

to be that of the C₂-symmetric complex **21** (Scheme 6), which was presumably derived from the *ortho*-methyl C–H activation of two ruthenium-coordinated NHC ligands in the presence of 2 equiv of methylenetriphenylphosphine (**23**) as a base.

A summary of the proposed decomposition pathway for catalyst **18** is depicted in Scheme 7. Although the methylidene **22** readily forms upon the exposure of **18** to ethylene, it appears to be more vulnerable to phosphine attack and subsequent decomposition relative to **5**, resulting in the minimal population (<2%) of **22** that had been observed during the course of the reaction. Differences in this decomposition route compared to that proposed for catalyst **5** potentially can be attributed to the weaker basicity and less steric hindrance of triphenylphosphine relative to tricyclohexylphosphine^{39,40} as well as the presence of ethylene in the reaction mixture.⁴¹

Decomposition of Phosphine-Free Catalysts. Catalyst **3** is known as a more stable catalyst than **2** under air and water due to the chelation of its isopropoxy ligand.^{42,43} However, as with the phosphine-containing catalysts, a comparison of stability between initiators is not particularly meaningful.^{15,22} Both catalysts **2** and **3** are thermally stable: their half-lives at 55 °C in benzene are over a month. Because the methylidene derivative of **3** cannot be isolated, its decomposition was examined directly in the presence of ethylene (Scheme 8). After 1 day, unidentified ruthenium hydride species were observed by ¹H NMR at -1.54 and -4.96 ppm. Attempts to isolate these species were unsuccessful. These species could be responsible for the olefin-isomerization reactions known to be catalyzed by **3**.^{13,14} This result suggests that other decomposition modes, which are only slightly slower than the phosphine-involved decomposition, are also available when a phosphine is not present.

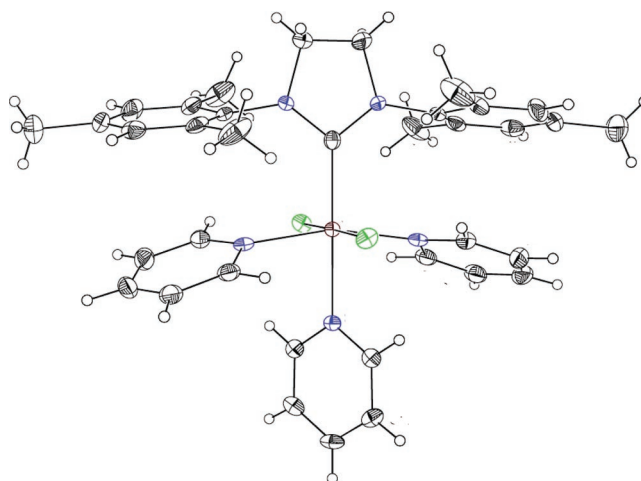


Figure 2. Crystal structure of (H₂IMes)(py)₃(Cl)₂Ru (**25**).

Bispyridine-based catalysts, such as **4**, have proven to be useful for the synthesis of polymers due to their fast-initiation rates.^{34,44} However, the lower stabilities of these catalysts limit their application. We tried to synthesize (H₂IMes)(py)₂(Cl)₂Ru=CH₂ (**24**) to compare with other methylidene complexes; however, any synthetic attempts were unsuccessful due to its instability. Even in situ, the methylidene protons of complex **24** were never observed by ¹H NMR.

Interestingly, complex **25** and methyltricyclohexylphosphonium chloride were formed from the reaction of **5** with an excess of pyridine (Scheme 9). The structure of **25** was determined by X-ray crystallography (Figure 2). All bond distances and angles in this structure are typical, but the mesityl groups are twisted by ~25° with respect to each other, which contrasts with their usual orientation perpendicular to the imidazolidine ring.

The formation of **25** was also observed during the reaction of **4** with ethylene in the absence of a PCy₃ ligand. Complex **25** also has been observed from the synthetic trials of a bulky chelating alkylidene from **4**.⁴⁵ Sponsler and co-workers reported a similar product from the decomposition of (H₂IMes)(3-bromopyridine)₂(Cl)₂Ru=CHR (R = Me, Et, *n*Pr).⁴⁶ Although they did not determine the structure of this decomposition product, their ¹H NMR data match those of **25**. These observations indicate that complexes similar to **25** typically form during the decomposition of pyridine-containing ruthenium olefin metathesis catalysts regardless of the presence of phosphines. The fate of the methylidene carbon is not clear in these or other cases where the [Ru]=CH₂ is generated in the presence of pyridines.⁴⁷

Conclusion

We have examined the decomposition of a series of ruthenium metathesis catalysts. Ruthenium methylidene complexes, the most common yet least stable isolable intermediate during olefin

(39) Zhang, X. M.; Bordwell, F. G. *J. Am. Chem. Soc.* **1994**, *116*, 968–972.

(40) Streitwieser, A.; McKeown, A. E.; Hasanayn, F.; Davis, N. R. *Org. Lett.* **2005**, *7*, 1259–1262.

(41) For a mechanistic investigation on the influence of phosphine on the rate of initiation of **2**, **5**, and **18**, see ref 23.

(42) Garber, S. B.; Kingsbury, J. S.; Gray, B. L.; Hoveyda, A. H. *J. Am. Chem. Soc.* **2000**, *122*, 8168–8179.

(43) Hong, S. H.; Grubbs, R. H. *J. Am. Chem. Soc.* **2006**, *128*, 3508–3509.

(44) Love, J. A.; Morgan, J. P.; Trnka, T. M.; Grubbs, R. H. *Angew. Chem., Int. Ed.* **2002**, *41*, 4035–4037.

(45) Hejl, A.; Grubbs, R. H. California Institute of Technology, Pasadena, CA. Unpublished work, 2006.

(46) Williams, J. E.; Harner, M. J.; Sponsler, M. B. *Organometallics* **2005**, *24*, 2013–2015.

(47) Methylpyridinium salt was not observed in the reaction of **4** in the presence of ethylene. Werner and coworkers have reported that a similar reaction between the ruthenium methylidene complex (PPri₂Ph)₂(CO)(Cl)(H)Ru=CH₂ and pyridine yields (PPri₂Ph)₂(py)(CO)(Cl)(H)Ru. See: Werner, H.; Stier, W.; Weberndörfer, B.; Wolf, J. *Eur. J. Inorg. Chem.* **1999**, 1707–1713.

metathesis, have been chosen as model complexes. All of the phosphine-containing methylidene complexes we examined decomposed following first-order kinetics to generate methylphosphonium salts. The observed kinetic behavior suggests that the major decomposition pathway involves attack of the dissociated phosphine on the methylidene carbon. Such a mechanism also explains the decomposition observed in the presence of ethylene as a model olefin substrate. The novel ruthenium ethylene complex **21** was observed from the decomposition of the catalyst **18** under ethylene. The decomposition of phosphine-free catalyst **3** generated unidentified ruthenium hydride species under an atmosphere of ethylene. Attempts to synthesize a pyridine-coordinated analogue of methylidene **4** were unsuccessful, presumably due to rapid decomposition. Instead, we observed the tris(pyridine) complex **25** as a decomposition product. This decomposition study will provide rational basis to design and synthesize more efficient ruthenium olefin metathesis catalysts.

Experimental Section

General Considerations. Manipulation of organometallic compounds was performed using standard Schlenk techniques under an atmosphere of dry argon or in a nitrogen-filled Vacuum Atmospheres dry box ($O_2 < 2.5$ ppm). NMR spectra were recorded on a Varian Inova (499.85 MHz for 1H ; 202.34 MHz for ^{31}P ; 125.69 MHz for ^{13}C) or on a Varian Mercury 300 (299.817 MHz for 1H ; 121.39 MHz for ^{31}P ; 74.45 MHz for ^{13}C). ^{31}P NMR spectra were referenced using H_3PO_4 ($\delta = 0$ ppm) as an external standard. Elemental analyses were performed at Desert Analytics (Tucson, AZ). Mass spectra were recorded on JEOL JMS 600H spectrophotometer. Silica gel used for purification of organometallic complexes was obtained from TSI Scientific, Cambridge, MA (60 Å, pH 6.5–7.0). Benzene, benzene-*d*₆, pentane, diethyl ether, THF, and methylene chloride were dried by passage through solvent purification columns. CD_2Cl_2 was dried by vacuum transfer from CaH_2 . All solvents are degassed by either a generous Ar sparge or three freeze–pump–thaw cycles. Catalysts **1**, **2**, and **3** were obtained from Materia Inc. and used as received. Ruthenium complexes **4**,³⁴ **5**,²³ **13**,⁴⁸ **18**,²³ and $(H_2IMes)(PCy_3)(Br)_2Ru=CHPh^{23}$ were prepared according to literature procedures. Methyltriphenylphosphonium chloride was purchased from Aldrich.

$(PCy_3)_2(Br)_2Ru=CH_2$ (9**).** A solution of **1** (166 mg, 0.182 mmol) in CH_2Cl_2 (3 mL) was stirred under an atmosphere of ethylene for 30 min at room temperature. The solvent was removed under vacuum, and the residue was repeatedly washed with cold pentane (5 mL) and dried under vacuum. A burgundy microcrystalline solid (146 mg, 0.175 mmol, 96%) was obtained. 1H NMR (C_6D_6): δ 19.38 (s, 2H), 3.00–2.80 (m, 6H), 1.95–1.20 (all m, 60H). $^{13}C\{^1H\}$ NMR (CD_2Cl_2): δ 297.3 (t, $J_{CP} = 8.2$ Hz), 31.6 (t, $J_{CP} = 10.1$ Hz), 29.7 (s), 28.0 (t, $J_{CP} = 5.1$ Hz), 26.8 (s). $^{31}P\{^1H\}$ NMR (C_6D_6): δ 44.51 (s). HRMS analysis (FAB) *m/z*: Calcd for $C_{37}H_{68}Br_2P_2Ru$ [M^+] 836.2199, found 836.2174.

$(H_2IMes)(PCy_3)(Br)_2Ru=CH_2$ (10**).** A solution of $(H_2IMes)(PCy_3)(Br)_2Ru=CHPh$ (300 mg, 0.320 mmol) in C_6D_6 (5 mL) was stirred under an atmosphere of ethylene for 90 min at 50 °C. The brown solution was cooled to room temperature, and the product was purified by column chromatography (gradient elution: 100% pentane to 8:1 pentane/diethyl ether) to afford an orange-yellow solid (95 mg, 0.110 mmol, 34%). 1H NMR (C_6D_6): δ 18.53 (s, 2H), 6.89 (s, 2H), 6.73 (s, 2H), 3.26 (m, 4H), 2.80 (s, 6H), 2.65–2.47 (m, 3H), 2.63 (s, 6H), 2.17 (s, 3H), 2.09 (s, 3H), 1.80–1.00 (m, 30H). $^{13}C\{^1H\}$ NMR (C_6D_6): δ 296.7 (d, $J_{CP} = 10$ Hz), 221.8 (d, $J_{CP} = 74.8$ Hz), 138.8, 138.4, 138.0, 137.6, 137.1, 134.9, 130.7, 130.1, 129.8, 129.6, 128.4,

127.8, 51.7 (d, $J_{CP} = 3.5$ Hz), 31.3, 31.0, 30.8, 29.3, 27.9, 27.8, 26.5, 21.0 (d, $J_{CP} = 2.6$ Hz), 20.9, 19.7. $^{31}P\{^1H\}$ NMR (C_6D_6): δ 38.02 (s). Anal. Calcd for $C_{40}H_{61}N_2Br_2PRu$: C, 55.75; H, 7.13; N, 3.25. Found: C, 56.04; H, 7.13; N, 3.25.

$(H_2IPr)(PCy_3)(Cl)_2Ru=CH_2$ (11**).** A solution of $(H_2IPr)(PCy_3)(Cl)_2Ru=CHPh$ (300 mg, 0.321 mmol) in C_6D_6 (5 mL) was stirred under an atmosphere of ethylene for 30 min at 45 °C. The brown solution was cooled to room temperature, and the product was purified by column chromatography (gradient elution: 100% pentane to 12:1 pentane/diethyl ether) to afford an orange-yellow solid (95 mg, 0.110 mmol, 34%). This product was very air-sensitive, and even slowly decomposed in the dry box. Further study was done immediately after the synthesis. 1H NMR (C_6D_6): δ 18.22 (s, 2H), 7.22–7.09 (m, 11H), 4.10 (m, 2H), 3.74–3.60 (m, 6H), 2.37–2.20 (m, 3H), 1.70–0.96 (m, 54H). $^{13}C\{^1H\}$ NMR (C_6D_6): δ 294.8 (d, $J_{CP} = 8.3$ Hz), 224.2 (d, $J_{CP} = 75.7$ Hz), 150.1, 148.7, 137.9, 136.2, 130.9, 130.0, 128.9, 128.7, 128.5, 128.3, 125.1, 124.9, 55.2, 53.6, 31.2, 31.0, 29.6, 29.5, 28.8, 28.3, 28.3, 27.6, 27.0, 25.2, 24.3. $^{31}P\{^1H\}$ NMR (C_6D_6): δ 38.83 (s). HRMS analysis (FAB) *m/z*: Calcd for $C_{46}H_{73}N_2Cl_2RuP$ [M^+] 856.3932, found 856.3917.

$(H_2IMes)(py)_3(Cl)_2Ru$ (25**).** A solution of **5** (150 mg, 0.195 mmol), excess pyridine (0.25 mL), and 1.0 mL of toluene was stirred at room temperature for 30 min. A 20 mL portion of hexanes was added, and the solution was allowed to sit without stirring for 3 min. The red solution was decanted away from the pale yellow precipitate and cooled to 0 °C. The resulting red precipitate was collected and redissolved in a minimum amount of toluene. Again, 20 mL of hexanes was added, the solution cooled, and the red precipitate collected. This procedure was repeated three more times. Finally, the precipitate was dried under vacuum to provide 0.041 g (mmol, 29%) of **25** as a red-orange solid. 1H NMR (CD_2Cl_2): δ 9.00 (d, $J = 5.5$ Hz, 4H), 8.70 (d, $J = 5.5$, 2H), 7.30 (t, $J = 7.5$ Hz, 1H), 6.98 (t, $J = 7.5$ Hz, 2H), 6.76 (t, $J = 7.0$ Hz, 2H), 6.34 (s, 4H), 6.33 (t, $J = 7.0$, 4H), 3.98 (s, 4H), 2.47 (s, 12H), 2.02 (s, 6H). $^{13}C\{^1H\}$ NMR (C_6D_6): δ 198.2, 142.2, 138.5, 128.4, 125.6, 125.0, 123.1, 120.3, 118.4, 113.1, 118.9, 54.1, 25.7, 24.5. HRMS analysis (FAB) *m/z*: Calcd for $C_36H_{41}N_5Cl_2Ru$ [M^+] 715.1783, found 715.2783.

Procedure for a Typical Decomposition Measurement. A 0.0161 mmol portion of methylidene and ~0.00561 mmol of anthracene were weighed into a 1 dram vial. A 700 μ L volume of benzene-*d*₆ was used to transfer the sample to a screw-cap NMR tube. A screw-cap was used to seal the NMR tube, and this seal was reinforced with Parafilm. The sample was placed into the spectrometer and allowed to equilibrate at the probe temperature for 10 min. Complex decomposition was following by monitoring the diminution of the methylidene protons through collection of a time-delayed array of 1H NMR spectra (referred to as a preacquisition delay, PAD, by Varian software). Plots of [methylidene] versus time and ^{31}P spectra of the decompositions are shown in Charts S.1–S.4 and Figures S.1–S.5 (Supporting Information).

Decomposition of **18 with Ethylene.** In a N_2 -filled glovebox, a J-Young tube was charged with complex **18** (17.5 mg, 0.021 mmol, 1.0 equiv) and 600 μ L of a stock solution containing 0.014 M anthracene (1.5 mg, 0.0084 mmol) in CD_2Cl_2 , yielding a homogeneous brown solution. The tube was sealed with a Teflon stopper, removed from the box, and attached to a Schlenk line. The tube was cooled to –78 °C, placed under vacuum (100 mTorr), and then backfilled with an atmosphere of ethylene. The tube was sealed, shaken, and allowed to warm to 23 °C. Reaction progress was monitored by 1H NMR (300 MHz) at 23 °C, observing the disappearance of **18** ($\delta = 19.21$ ppm, $Ru=CHPh$) and the appearance of complex **11** ($\delta = 18.59$, $Ru=CH_2$). These results are depicted in Chart S.5 (Supporting Information).⁴⁹

Mass Spectrometric Analysis of the Decomposition Reaction of **18 with Ethylene.** To an NMR tube equipped with a Teflon screw

(48) Schwab, P.; Grubbs, R. H.; Ziller, J. W. *J. Am. Chem. Soc.* **1996**, *118*, 100–110.

(49) The alkylidene was assumed to be methylidene-derived (2H); values should be doubled when calculating conversion to **11** relative to ruthenium because it is a bimetallic species.

Table 2. Summary of Crystallographic Data for **7**, **21**, and **25**

	7	21	25
formula	[C ₁₉ H ₃₆ P] ⁺ Cl ⁻ ·3(H ₂ O)	C ₄₆ H ₅₈ N ₄ Cl ₂ Ru ₂	C ₃₆ H ₄₁ N ₅ Cl ₂ Ru
<i>M</i> _r	384.95	940.00	715.71
cryst color	colorless	red/brown	orange
cryst size (mm ³)	0.30 × 0.23 × 0.18	0.21 × 0.18 × 0.07	0.33 × 0.28 × 0.08
cryst syst	triclinic	triclinic	orthorhombic
space group	<i>P</i> 1	<i>P</i> 1	Pbcn
<i>a</i> (Å)	9.8774(4)	9.8735(6)	11.3376(7)
<i>b</i> (Å)	10.0035(5)	10.7053(7)	13.3755(8)
<i>c</i> (Å)	12.7700(6)	11.8315(7)	21.4203(14)
α (deg)	85.1580(10)	100.828(2)	90
β (deg)	74.3040(10)	98.018(2)	90
γ (deg)	63.5350(10)	116.4470(10)	90
<i>V</i> (Å ³)	1086.48(9)	1063.77(11)	3248.3(4)
<i>Z</i>	2	1	4
<i>D</i> _{calcd} (g cm ⁻³)	1.177	1.467	1.463
<i>T</i> (K)	100(2)	100(2)	98(2)
λ (Å)	0.71073	0.71073	0.71073
μ (mm ⁻¹)	0.263	0.872	0.681
R1 ^a (all data)	0.0618	0.0724	0.0481
wR2 ^b (all data)	0.0772	0.0714	0.0509
GOF	1.307	1.146	1.716

$$^a R1 = \sum ||F_o| - |F_c|| / \sum |F_o|. \quad ^b wR2 = [\sum w(F_o^2 - F_c^2)^2 / \sum w(F_o^2)]^{1/2}.$$

cap in the glovebox, complex **18** (17.5 mg, 0.021 mmol, 1.0 equiv) was dissolved in 600 μL of CD₂Cl₂, forming a homogeneous brown solution. The tube was sealed, removed from the box, and attached to a Schlenk line. The tube was then cooled to -78 °C, placed under vacuum (100 mTorr), and backfilled with an atmosphere of ethylene. The NMR tube was removed from the Schlenk line, shaken, and allowed to warm to 23 °C. Mass spectrometric analysis at 8 min revealed the presence of a ruthenium complex possessing the same calculated mass as **11** (Figure S.6, Supporting Information): (FAB⁺) *m/z* 971.1 (M - H);⁵⁰ Analysis of the reaction mixture after 24 h via ¹H NMR, ³¹P NMR, and HRMS confirmed the presence of methyltriphenylphosphonium chloride (**20**) via correlation to authentic material (Figure S.7, Supporting Information).

Reaction of 18 with Ethylene to Generate Metallocyclobutane 19. To a J-Young tube in the glovebox, complex **18** (17.5 mg, 0.021 mmol, 1.0 equiv) was dissolved in 600 μL of a stock solution containing 0.014 M anthracene (1.5 mg, 0.0084 mmol) in CD₂Cl₂, forming a homogeneous brown solution. The tube was sealed with a Teflon stopper, removed from the box, and attached to a Schlenk line. The tube was then cooled to -78 °C, placed under vacuum (100 mTorr), and backfilled with an atmosphere of ethylene. The tube was sealed, shaken, and allowed to warm to 23 °C. The reaction was monitored via ¹H NMR (500 MHz) at 23 °C for 20 min, at which time complex **18** was over 90% consumed and **11** was the predominant alkylidene species (~44% yield relative to Ru). The reaction was then cooled to -40 °C. After 3 h at -40 °C, the peak at 18.59 ppm (corresponding to complex **11**) had completely diminished, and two new peaks at 6.64 ppm (4H) and -2.63 ppm (2H) were clearly visible, corresponding to the literature values for the α- and β-hydrogens of ruthenium metallocycle **19**.^{36,37}

Decomposition Products of 18. To a 10 mL Schlenk tube in the glovebox, complex **18** (56 mg, 0.077 mmol, 1.0 equiv) was dissolved in 2.2 mL of toluene, forming a homogeneous brown solution. The tube was sealed with a Teflon stopper, removed from the box, and attached to a Schlenk line. The tube was then cooled to -78 °C, placed under vacuum (100 mTorr), and backfilled with an atmosphere of ethylene. The tube was sealed, shaken, and allowed to warm to 23 °C. The reaction was allowed to stand for 5 days at 23 °C. During this

time, a white solid (methyltriphenylphosphonium chloride, **20**) was observed to precipitate out of solution in addition to the formation of red-brown crystals. The Schlenk line was opened in the glovebox, and the toluene was carefully transferred out via syringe. The crystals were then washed with two 500 μL portions of a 50:50 toluene/pentane mixture. A 52 mg portion of the red-brown crystals was isolated and analyzed via X-ray crystallography and found to be complex **21**. Further spectroscopic analysis of **21** proved problematic, due to its instability in solution. ³¹P NMR analysis of both the white precipitate and mother liquor revealed the only phosphorus-containing product to be methyltriphenylphosphonium chloride (**20**).

X-ray Crystallographic Data Collection and Refinement. For compounds **7**, **21**, and **25** each crystal was mounted on a glass fiber using Paratone and placed in the cold stream of an Oxford Cryostream. Intensity data were collected on a Bruker SMART1000 diffractometer. The data were integrated using the Bruker SAINT (v6.45) program. Each crystal structure was solved by direct methods and then refined by full-matrix least-squares using Bruker SHELXTL. All non-hydrogen atoms were refined with anisotropic displacement parameters. Hydrogen atoms were located in the difference Fourier and refined isotropically without restraint except for the hydrogen atoms on water in compound **7**, which were restrained as riding atoms. The crystallographic data are summarized in Table 2, and complete details are included in the Supporting Information.

Acknowledgment. The authors thank Dr. Mona Shahgholi for the mass spectrometric analyses, Lawrence M. Henling for contributions to the X-ray crystallography, and Andrew Hejl for generous donation of complex **25**. Materia, Inc. is acknowledged for generous donation of ruthenium catalysts **1–3**. Postdoctoral funding for A.G.W. was provided by the NIH (NRSA GM070147-02) and UNCF-Pfizer. This work was supported by the National Science Foundation.

Supporting Information Available: Kinetic plots, mass, ³¹P spectra, and crystallographic details and data in CIF format of **7**, **21**, and **25**. This material is available free of charge via the Internet at <http://pubs.acs.org>.

JA0713577

(50) The presence of **11** has also been observed via mass spectrometry in the reaction of the bispyridyl catalyst **4** with ethylene.